

EU Fifth Framework Programme 1998-2002
Energy, Environment and Sustainable Development

**Environmental Design of
Low Crested Coastal Defence Structures
(DELOS)**



Report

Deliverable D48

WP 3.5

Report on model of suitable habitats for key species on
breakwaters as a function of local hydrodynamics

Introduction.....	2
Direct hydrodynamical effects on epibiota in the wave-swept zone	4
Wave exposure: average and maximum flow speeds measured in the field	5
Wave exposure: wave buoy time series.....	6
Landward and seaward sides of LCS	6
Mechanistic model of wave-induced detachment of epibiota	8
Model strategy.....	8
Model results.....	11
Validation of model.....	12
Weakness of the hydrodynamic model.....	13
Effects of surface topography on epibiota.....	14
Large-scale topography: refuges.....	14
Small-scale topography: roughness.....	15
Scour.....	15
Water exchange and demand for oxygen and nutrients	17
Model of LCS interior flow and biological oxygen demand.....	17
Model of LCS interior flow and nutrient depletion	19
Statistical models of epibiotic distribution on LCS	20
General patterns of landward and seaward side differences.....	20
Patterns on smaller scales	23
Along LCS gradients	23
Horisontal and vertical rock faces.....	23
Conclusions.....	24
References cited.....	24
Appendix	25

Introduction

It is well established that the distribution of intertidal organisms are correlated to wave exposure (e.g. Lewis 1968). Exposure is rarely well defined and a number of measures have been used to quantify exposure. Most measures involve different aspects of fetch and dominating wind directions (Anonymous). Rarely has the effect of waves been directly measured (but see Denny 1988) and often exposure is classified in terms of the biological community, introducing logical circularity. Surprisingly little effort has been focused on cause-effect relationships behind the observed correlations between wave exposure and the distribution of organisms. A few successful attempts to unravel the effects of wave action on the survival of shore organisms show that some organisms are indeed limited in their distribution by the hydrodynamic forces imposed by, in particular, breaking waves (Denny 1988, Blanchette 1997).

A low-crested breakwater (LCS) introduces a strong gradient in wave exposure, mainly between the seaward and the landward side. This gradient is clearly seen in both measurements of average flow regimes using erosion of gypsum (Fig. 1) and maximum forces using drag probes (Fig. 2). Gradients in wave exposure may also occur on smaller scales depending on the design of the LCS. Different faces of the building blocks will likely be exposed to different flow speeds as shown from the LCS in Elmer (Fig. 3).

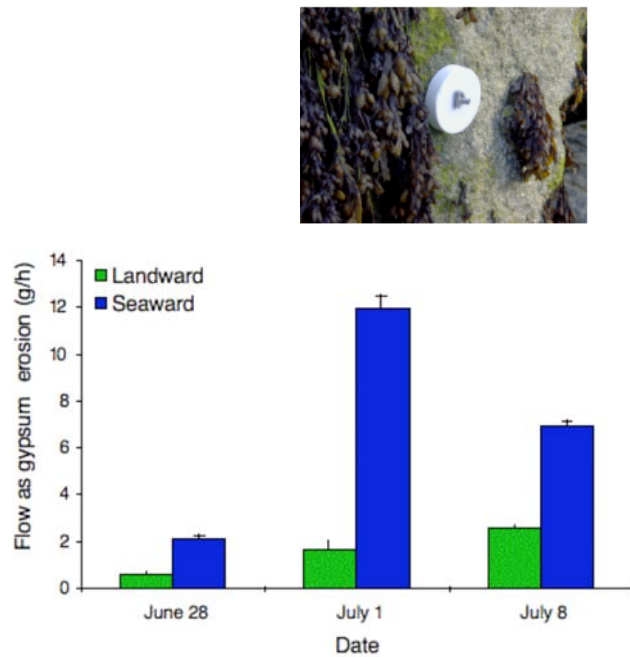


Fig. 1. Erosion of gypsum as a measure of average water motion. The photo inset shows a discs gypsum disc attached to an LCS in Elmer, UK. The graph shows the difference in erosion rates between the landward and the seaward side for 3 dates.



Fig. 2. Drag probes used to record maximum drag forces. For standardised measurements, allowing conversion to flow speeds, a training golf ball is used as a bluff body. The technique also allows the recording of maximum drag forces operating on individuals of *Fucus vesiculosus*.

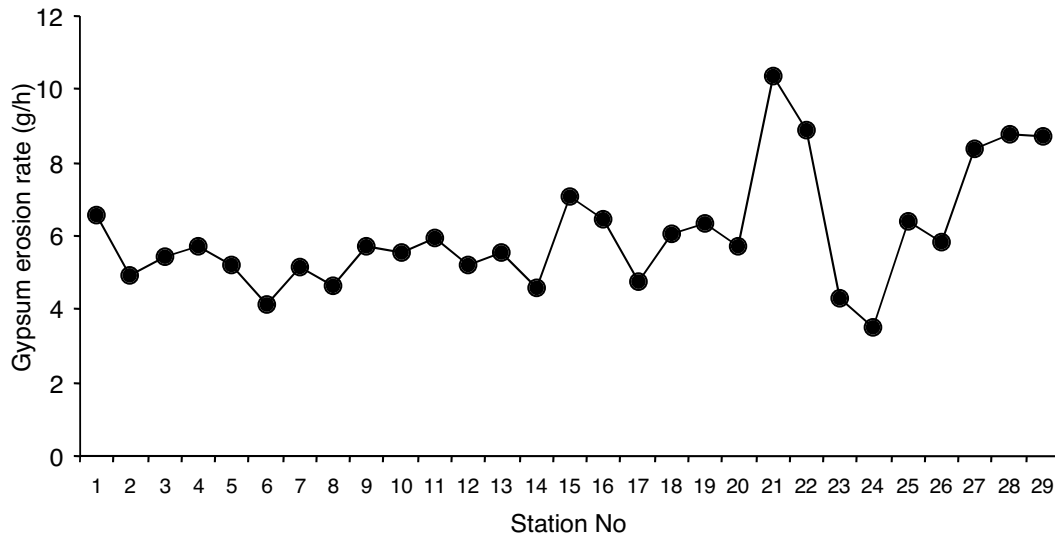


Fig. 3. Small-scale flow variation among individual building blocks on two LCS in Elmer, UK. The station No go from west to east. Flow is measured as the erosion of gypsum.

Within the DELOS program WP 3.5 has the objective to propose models that can predict suitable habitats for key species on breakwaters as a function of local hydrodynamics. Deliverable 48, reported here, focuses on the epibiota that may colonise the hard surfaces on and within LCS. The hydrodynamic regime may affect a number of factors that are important for the survival of epibiota on LCS. Within DELOS some of these factors have, hypothetically, been identified as particularly important. Below follows a description of these factors and possible ways to predict the survival of epibiota on LCS as a function of hydrodynamics.

Direct hydrodynamical effects on epibiota in the wave-swept zone

Waves exert a direct mechanical stress on organisms attached to surfaces. If this stress exceeds some critical level the organism may suffer tissue damages or complete removal, resulting in reduced growth or mortality. Critical stress levels likely change for different stages in the life cycle. A given stress level may inhibit larval settlement and thus recruitment for one species, while for another species the same stress level reduces the maximum size of the adult stage (Blanchette 1997).

The mechanical stress on an attached organism can be predicted from hydrodynamic theory. The stress is mainly caused by the flow speed and, in unsteady flow, flow acceleration. The hydrodynamic forces acting on a stationary organism can be separated into drag, acceleration reaction and lift. Hydrodynamic drag (f_d) is generally expressed as:

$$f_d = \frac{1}{2} \rho u^2 S_p C_d \quad \text{eq. 1}$$

where ρ is the water density, u is the flow speed, S_p is the projected area of the organism and C_d is the drag coefficient. In unsteady flow (as in waves) the flow is accelerating and decelerating and a second force, the acceleration reaction, will act together with the drag force. The acceleration reaction (f_a) is expressed as:

$$f_a = \rho C_m V a \quad \text{eq. 2}$$

where C_m is the inertia coefficient, V is the volume of the organism and a is the flow acceleration. In contrast to the drag force and the acceleration reaction, the lift force acts perpendicular to the flow direction. The lift force (f_l) is expressed as:

$$f_l = \frac{1}{2} \rho u^2 S_{plan} C_l \quad \text{eq. 3}$$

where S_{plan} is the planiform area (projected perpendicular to flow) and C_l is the lift coefficient. The overall net force (f_n) on a stationary organism is found by combining eq. 1-3 as:

$$f_n = \sqrt{(f_d + f_a)^2 + (f_l)^2} \quad \text{eq. 4}$$

and with the direction (ϕ):

$$\phi = \arctan\left(\frac{f_l}{f_d + f_a}\right) \quad \text{eq. 5}$$

Drag and lift forces on attached, inflexible organisms are often of similar magnitude, and the acceleration reaction may add significant force in breaking waves where convective turbulence results in large flow acceleration.

With the hydrodynamic expressions above it is possible to estimate the force acting on epibiota if the morphometrics of the organism is measured and if local flow speed and acceleration are known. These estimates may then be compared to measurements of adhesion forces or critical tissue breaking stress in order to predict dislodgement or damage in a particular flow regime (see below). As will be discussed below, the major difficulty is to obtain accurate measurements of flow speed on the scale of attached organisms and to include rare high-energy wave events.

Wave exposure: average and maximum flow speeds measured in the field

The sustained survival on a wave-exposed LCS is the result of the flow pattern integrated over the life-span of an organism, often covering several seasons. Hypothetically, rare events of maximum hydrodynamic forces determine the probability of detachment, while average flow conditions are likely to better predict larval settlement and delivery of nutrients. Other aspects of the flow pattern may also be important for survival, e.g. critical periods of very low flow speeds causing hypoxia and sedimentation. The expected complex dependence on flow regime for long-term survival thus points to the difficulty and ambiguity of characterising the flow regime on LCS for predictions of epibiotic assemblages.

As a first step in DELOS, wave flow in the field has been characterised by short-term (day) average flow speed and maximum flow speed. Average flow speed was measured using the weight loss of discs cast in gypsum (Fig. 1, diameter 10 cm, thickness 2.5 cm) (Porter et al. 2000). The gypsum discs were bolted to the surface of LCS building blocks at Elmer, UK and in the Adriatic Sea in Italy. Erosion of gypsum was calibrated to average flow speed in the field using an acoustic doppler current profiler (ADCP). Maximum force acting on an object in breaking waves was estimated using spring-loaded balls (Bell and Denny 1994, Fig. 2). Maximum force was also calibrated to flow speed in steady flow. Assuming no lift force and different scenarios of convective acceleration, the maximum flow speed in breaking waves was estimated from eq. 4.

In addition to the empirical measurements at the field sites described above, maximum flow speed in breaking waves were calculated using wave theory. First the height of a breaking wave (H_b) can be found as (Goda 1985):

$$H_b = 0.18L_0 \left(1 - \exp \left[-1.5 \frac{\pi h}{L_0} (1 + 15\beta^{4/3}) \right] \right) \quad \text{eq. 6}$$

where L_0 is the deep-water wave length, h is the water depth and β is the beach slope. The maximum flow velocity (u_{max}) associated with the breaking wave is then calculated as (Denny 1988):

$$u_{max} = \sqrt{2gH_b} \quad \text{eq. 7}$$

where g is the acceleration of gravity. To determine if an approaching deep-water wave will break on the LCS or if it will break in the shallow water off-shore of the LCS an expression is needed for the wave shoaling, i.e. the transition from deep-water waves to shallow-water waves. A simple expression (linear wave theory) is (Denny 1988):

$$H = H_0 \sqrt{\frac{\sinh(2kh)}{\sinh(2kh) + 2kh} \frac{1}{\tanh(kh)}} \quad \text{eq. 8}$$

where H is the shallow-water wave height, H_0 is the deep-water wave height and k is $2\pi/L_0$.

Wave exposure: wave buoy time series

A major problem in predictions of long-term wave-induced forces on epibiota is that maximum forces occur only at rare events, mainly after storms. Simultaneously with the field measurements on the Elmer LCS deep-water waves were monitored using data from a wave buoy (NDBC 62305) 44 km south of the Elmer site. Deep-water wave patterns were then correlated to measured flow velocities in breaking waves. This information was then combined with historical time series from a wave buoy (BODC, Owers) 19 km from the Elmer field site (UK) to cover extreme events.

Landward and seaward sides of LCS

The purpose of the LCS is to absorb wave energy and this leads to a drastic change in wave exposure going from seaward to the landward side. Measurements with gypsum discs clearly show that the average flow velocities decrease on the landward side. Figure 1 shows average loss of gypsum for the Elmer site in UK and Fig. 4 shows data from two sites in the Adriatic Sea, Italy. The tall ‘‘LCS’’ at Elmer is very close to shore resulting in a more marked difference between landward and seaward sides compared to the more distant and lower LCS in the Adriatic sea.

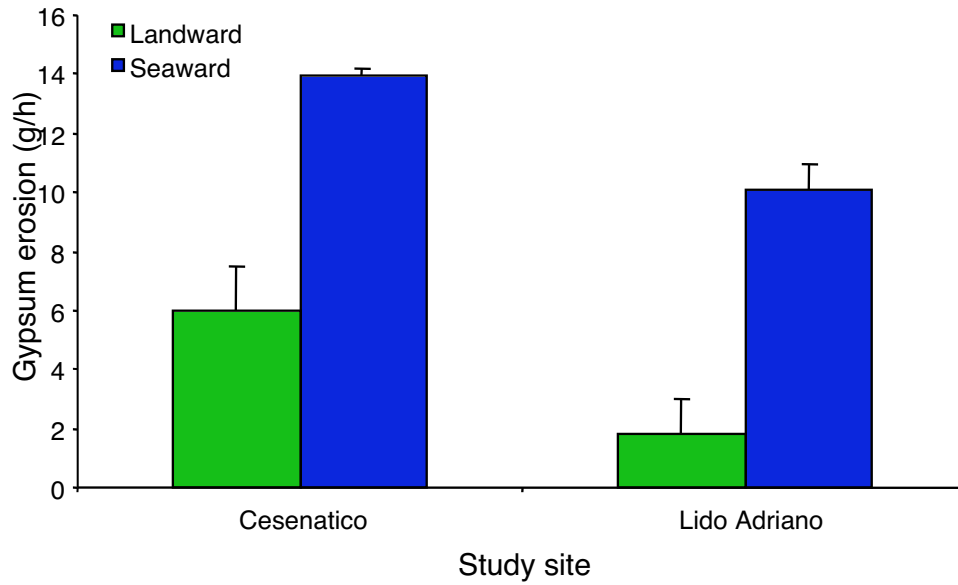


Fig. 4. Average flow speeds, measured as erosion of gypsum, for the landward and the seaward side of LCS at two sites on the Adriatic coast in Italy.

At the Elmer site the maximum flow speed calculated from maximum drag on spring-loaded bluff bodies (spheres) show a similar picture as for the gypsum loss. Figure 5 shows the maximum flow speeds measured at the Elmer site on the seaward and the landward sides.

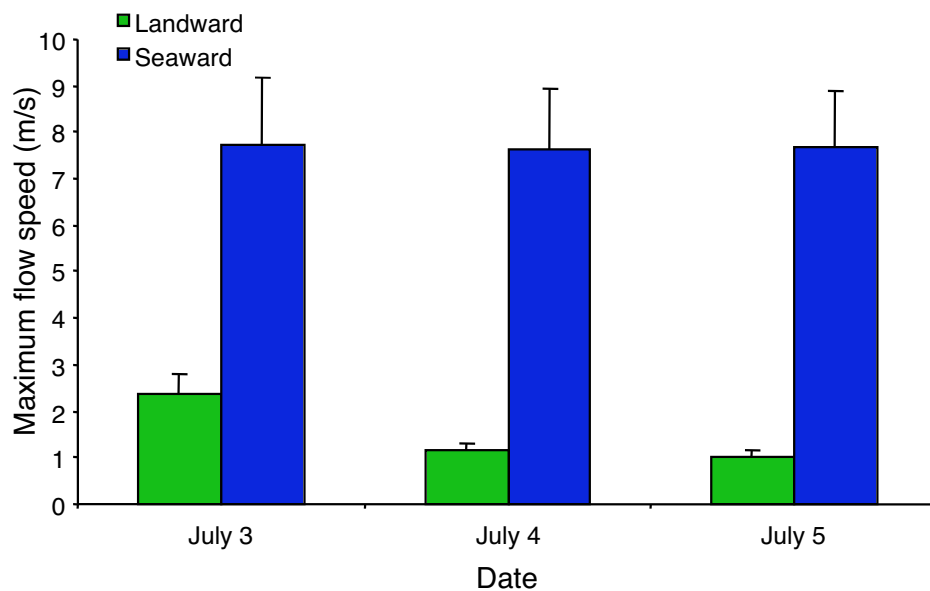


Fig. 5. Maximum flow speeds on landward and seaward sides of LCS in Elmer, UK. Maximum drag forces were recorded with drag probes during three days and converted to flow speeds.

Mechanistic model of wave-induced detachment of epibiota

Model strategy

The probability of wave-induced detachment of epibiotic organisms may be modelled if the hydrodynamic forces due to wave motion and the adhesion strength of the organism are known. The adhesion strength (tenacity) was directly measured for two key species at the Elmer site. The selected key species were *Fucus vesiculosus* representing large foliose macro-algae and *Littorina littorea* representing macrofauna (Fig. 6).



Fig. 6. Photos showing (A) *Littorina littorea* among the barnacle *Semibalanus balanoides*, and (B) an LCS block with *Enteromorpha* sp. on the top and *Fucus vesiculosus* hanging from the facing side.

The model strategy can be divided into the following steps:

1. Wave flow speeds were calculated from a historical time series of wave buoy data. Figure 7 shows significant wave height and period from the BODC station Owers. Using eq. 8 the height of the shoaling wave was calculated. For the relevant depth and slope the breaking wave height is calculated and compared with the shoaling wave height. If the wave breaks off-shore of the LCS the maximum flow speed is set to zero, just indicating low flow speeds. If the shoaling wave height is lower than breaking wave height the wave is assumed to break onto the LCS.

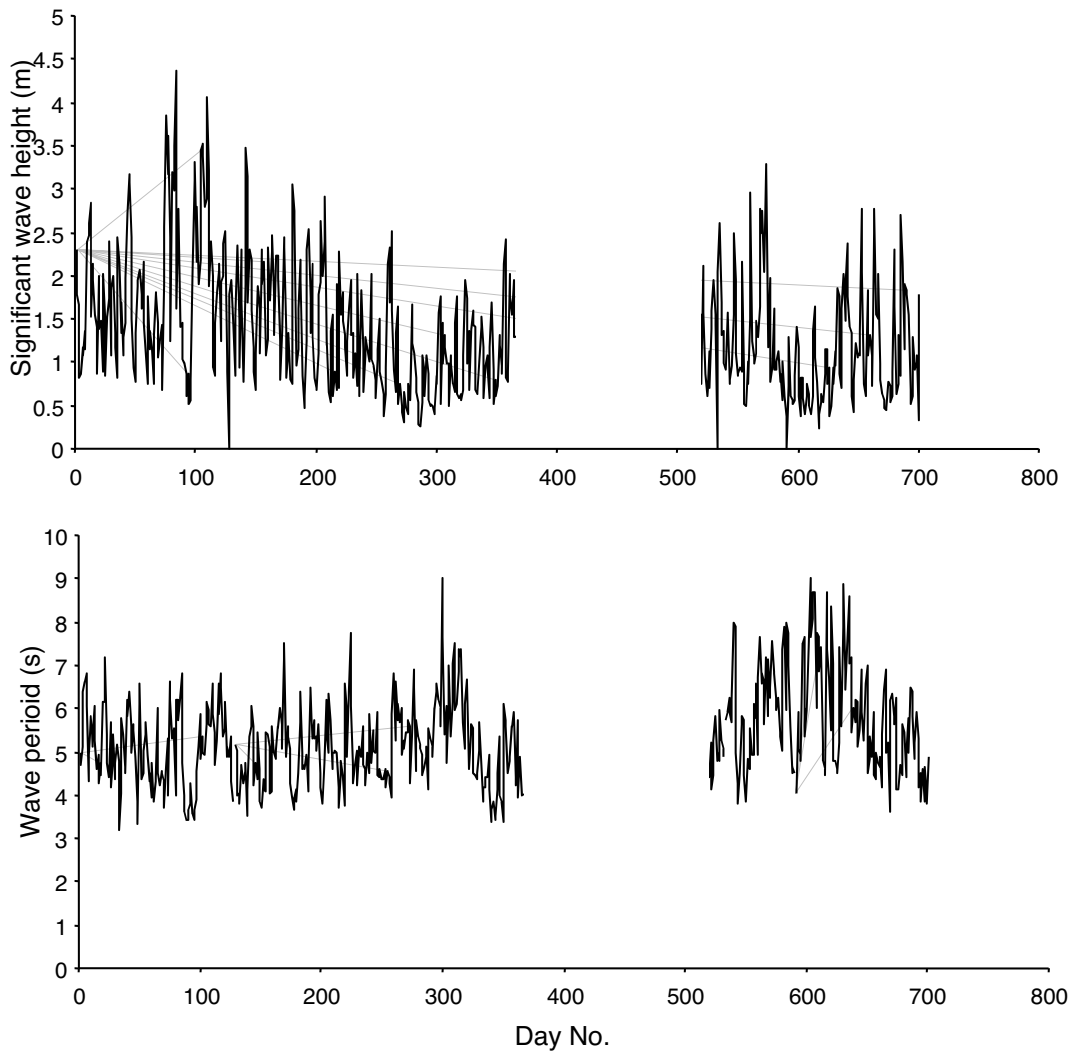


Fig. 7. Time series from Owers Lightship Vessel showing significant wave height and period. The time series spans from October 1968 to September 1970.

2. The maximum flow speed of the breaking wave is calculated from eq. 7.
3. The total hydrodynamic force acting on *Fucus vesiculosus* is assumed to be the sum of the drag force and the acceleration reaction. Lift force is assumed to be insignificant because the thallus is mainly exposed to symmetric cross-flow gradients because of the alignment with the flow direction.
4. For the force acting on *Littorina littorea* drag, lift and acceleration reaction forces are all evaluated using eq. 4.
5. No data exists on the flow acceleration (necessary to calculate acceleration reaction force). This is unfortunate since flow acceleration can be very high in breaking waves in relation to a fixed object leading to high acceleration reaction forces. Denny (1985) estimated flow accelerations as high as 2000 m s^{-2} during winter storms. The model considers a range of flow accelerations from $20\text{-}100 \text{ m s}^{-2}$ on the landward side and $100\text{-}400 \text{ m s}^{-2}$ on the seaward side.
6. Finally, the wave-induced forces are compared to the adhesion strength found empirically. Adhesion strengths of *Fucus vesiculosus* and *Littorina littorea* were measured using a spring-loaded dynamometer. Individual organisms were tethered with a thread and the force necessary to remove the organism (or break any tissue)

from the LCS surface was recorded. Figure 8 shows the critical breaking stresses for *Fucus vesiculosus* and Fig. 9 for *Littorina littorea*. For *Fucus* the breaking stress increases with frond size. *Littorina*, interestingly, showed significantly stronger adhesion on the seaward compared to the landward side.

7. The complete model was formulated in MatLab code (see Appendix A).

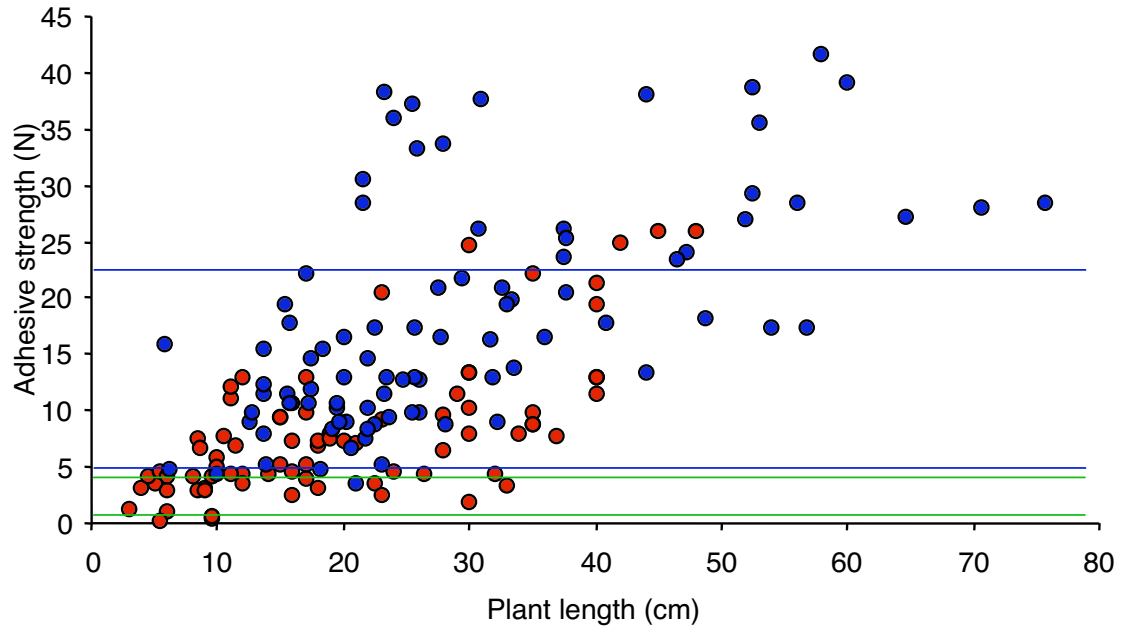


Fig. 8. The breaking force necessary to detach plants of *Fucus vesiculosus*. Red markers indicate data from Elmer and the blue markers indicate data from Sweden. The green and blue lines show the interval of modelled maximum wave-induced forces on the landward and the seaward sides, respectively, on LCS in Elmer, UK.

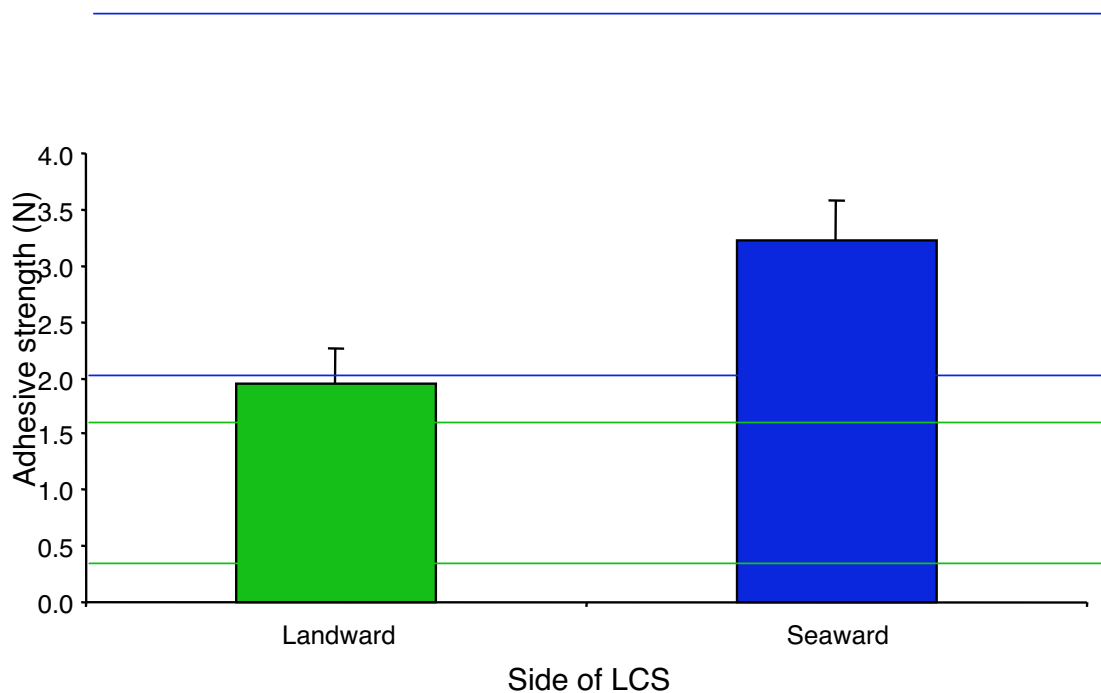


Fig. 9. The breaking force necessary to detach individuals of *Littorina littorea*. The green and blue lines show the interval of modelled maximum wave-induced forces on the landward and the seaward sides, respectively, on LCS in Elmer, UK.

Model results

Figure 10 shows the modelled forces acting on *Fucus vesiculosus* and Fig. 11 on *Littorina littorea* for both the seaward and the landward sides on Elmer LCS. The graphs show the span between a low and a high flow acceleration scenario. The model predicts that only very large *Fucus vesiculosus* have adhesion forces higher than the wave-induced forces on the seaward side (Figs. 8 and 10). On the landward side most individuals are expected to remain attached. For *Littorina littorea* a similar picture emerges where adhesion strength is only predicted to keep individuals securely attached on the landward side.

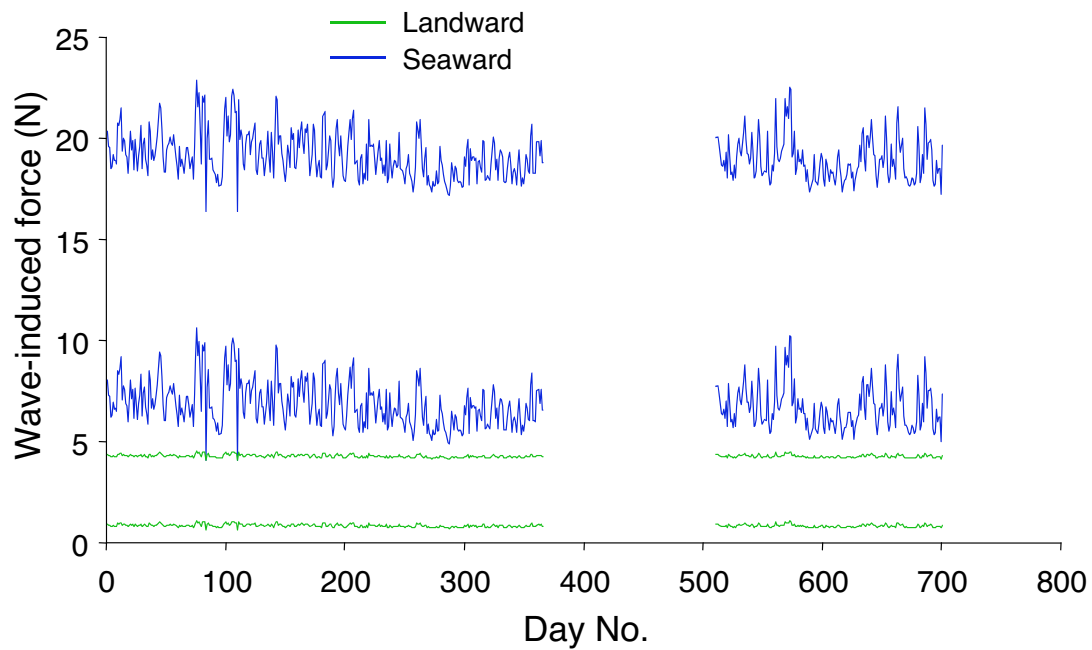


Fig. 10. Modelled wave-induced forces acting on *Fucus vesiculosus*. Blue indicates forces on the seaward side where the bottom and top time series assume maximum flow accelerations of 100 and 400 m s^{-2} , respectively. Green indicates forces on the landward side where the bottom and top time series assume maximum flow accelerations of 20 and 100 m s^{-2} , respectively.

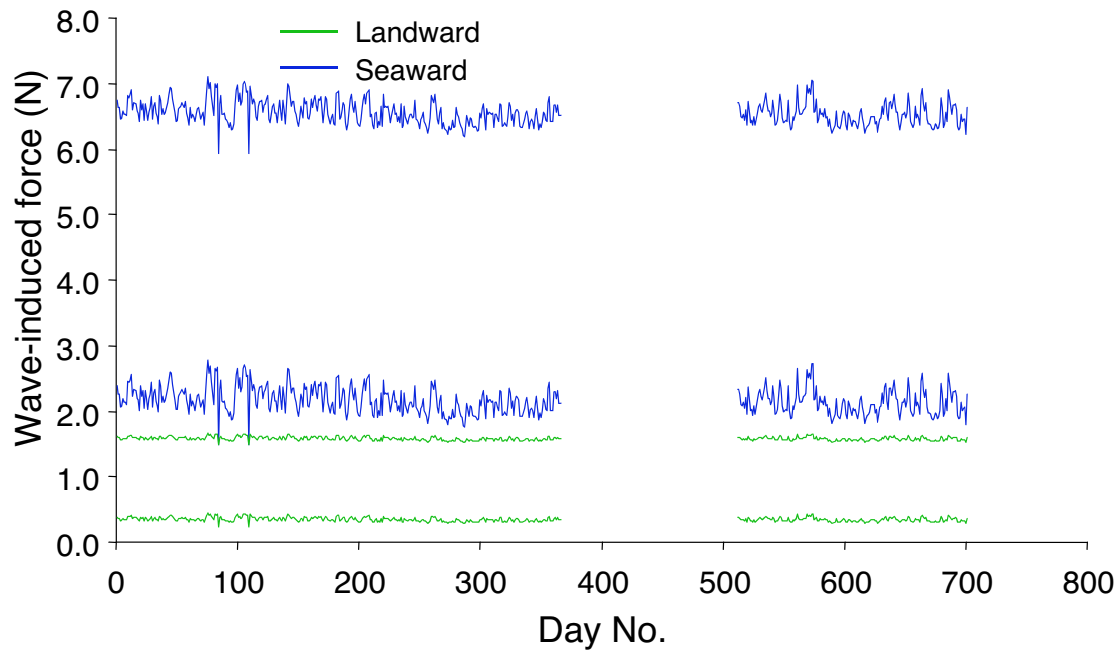


Fig. 11. Modelled wave-induced forces acting on *Littorina littorea*. Blue indicates forces on the seaward side where the bottom and top time series assume maximum flow accelerations of 100 and 400 m s^{-2} , respectively. Green indicates forces on the landward side where the bottom and top time series assume maximum flow accelerations of 20 and 100 m s^{-2} , respectively.

Validation of model

The strongest validation is of course that the predicted patterns, no *Fucus vesiculosus* and *Littorina littorea* on the seaward side of LCS, correspond to what is found in the field. Validation of the model was also performed in two more formal ways. Firstly, total wave-induced forces were directly measured for *Fucus vesiculosus* in Elmer. Secondly, a transplantation experiment was performed to test if *Fucus vesiculosus* is indeed detached (or torn apart) on the seaward side of LCS, as predicted from the hydrodynamic model. Direct measurements of the drag and acceleration reaction forces on *Fucus vesiculosus* corresponded reasonably well with model predictions, assuming a flow acceleration of 100 m s^{-2} (Fig. 12). Figure 13 shows the results of the transplantation experiment where individuals of *Fucus vesiculosus* were moved either to a new seaward side or a new landward side. Clearly, *Fucus* soon disappear from the seaward side while many individuals remained on the landward side, further supporting the model predictions. Also, many individuals decreased in frond size on the seaward side indicating tissue damages and mechanical wear.

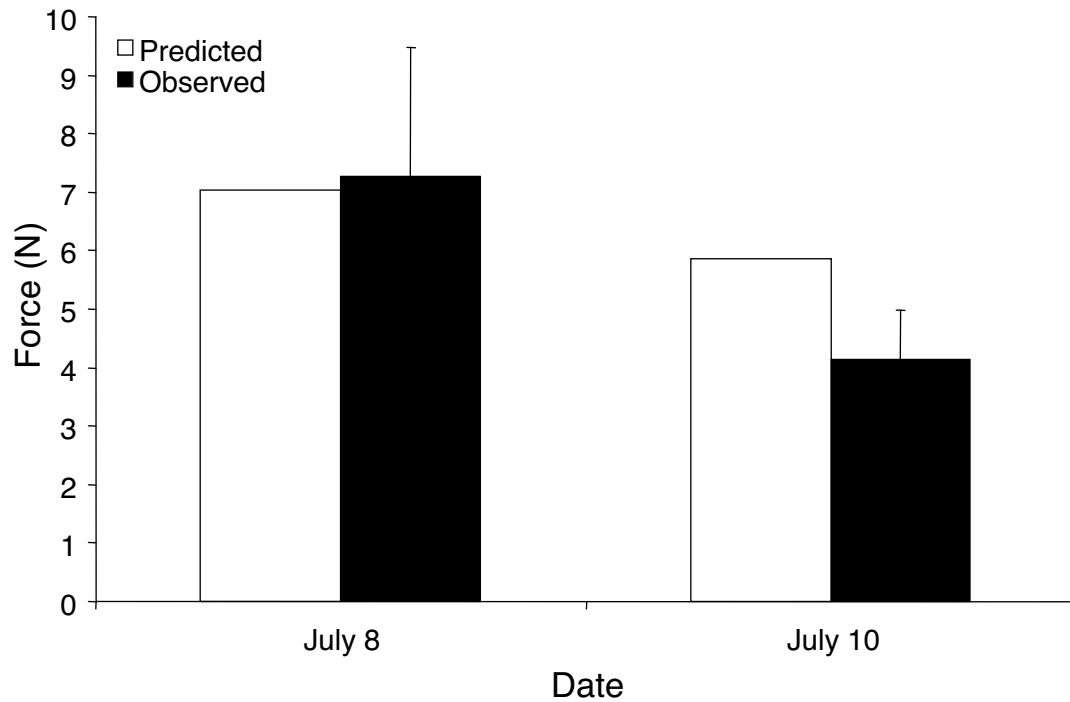


Fig. 12. Predicted maximum wave-induced forces acting on *Fucus vesiculosus* on the landward side of LCS compared with observed forces recorded in Elmer, UK on two dates. A flow acceleration of 100 m s^{-2} was assumed.

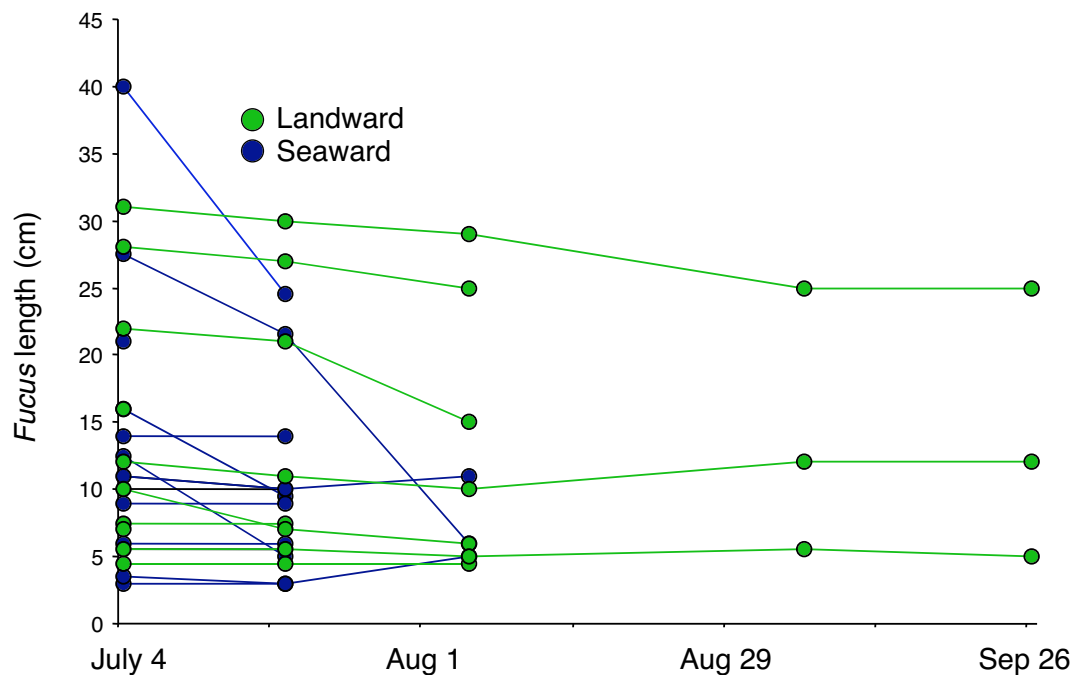


Fig. 13. Results from transplantation of *Fucus vesiculosus* to landward and seaward sides of LCS in Elmer, UK. The graph shows how the length of plants develop through time. Interrupted time series indicate detachment.

Weakness of the hydrodynamic model

There are several problems with the proposed hydrodynamic model to predict detachment of epibiota. The major weaknesses are thought to be:

1. Denny et al. (2003) have recently shown the difficulty in predicting maximum flow speeds in breaking waves. At present, theoretical predictions seem to underestimate maximum flow speeds, possibly because of interactions with local topography. The maximum forces predicted by the model are thus expected to underestimate forces during extreme conditions.
2. The distribution of wave heights approach the Rayleigh distribution. Assuming this distribution it is possible to predict the probability of a given wave height as:

$$P_{(H>H')} = \exp\left(-\left[\frac{H'}{0.71H_s}\right]^2\right) \quad \text{eq. 9}$$

where $P(H>H')$ is the probability that a wave is taller than some wave height A' for a wave climate characterised by the significant wave height H_s . For the most wavy period in Elmer (10 days in December) there will be approximately 144000 waves assuming a wave period of 6 s. The average significant wave height was 3.1 m during this time interval. According to eq. 9 the maximum wave height for this time interval is expected to be 7.5 m. Clearly, these waves will lead to considerably larger forces than predicted by the present model.

3. The model does not consider the presence of refuges offered by the LCS topography. Small epibiota, e.g. juvenile *Littorina littorea* and seedlings of *Fucus vesiculosus* may hide in crevices and thus escaping much of hydrodynamic forces. In a section below topographic effects are treated in more detail.
4. It is important to realise that although the hydrodynamic model correctly predicts that no *Fucus vesiculosus* occurs on the seaward side of LCS, the hydrodynamics may not actually cause this pattern. It is well known that the presence of grazing limpets (*Patella* spp.) can almost totally remove all seedlings of macroalgae. Within DELOS a field experiment is currently running to separate the effects of grazing and the effect of wave-induced forces on the presence of *Fucus vesiculosus*. The results are expected during the autumn of 2003.

Effects of surface topography on epibiota

Apart from the large-scale effects of landward and seaward sides of LCS there may be also be differences on smaller scales. The most important small-scale features are probably the differences in topography on and among the building-blocks of LCS. Several effects of topography on epibiota are possible depending on the scale and geometry of topographic elements. Topography on scales larger than an organism may offer protection from wave-induced forces, but also from predators, e.g. limpets. Topography smaller than the organism may interact with adhesion strength and ability to move or feed on the substratum.

Large-scale topography: refuges

Some LCS have large-scale topographic feature, e.g. gaps between armour building blocks, probably offering refuges for many epibiota. In WP 3.2 a manipulative experiment in Elmer, UK (deliverable D35) has shown that topographic features can significantly increase the abundance on the seaward side of, e.g. *Littorina* snails, *Mytilus* (mussels) and *Enteromorpha* (macro-algae). The prediction from Elmer is that topographic features on scales from a few mm to several cm can significantly increase the biodiversity on LCS. A general conceptual model is that holes or small basins in the LCS surface offer refuges from hydrodynamic forces, grazing and if horizontally

oriented prevents desiccation leading to more micro-environments allowing for a broader range of organisms.

Small-scale topography: roughness

Small-scale topographic elements are small in comparison to the target organism and may be termed texture or roughness. Many organisms respond to texture during larval or spore settling. Note that texture for an adult individual may be regarded as large-scale topography for a larva of the same species. Thus apparent texture may offer refuge from hydrodynamics and grazing for the early, small life stages. Many larvae actively select surfaces with sub-millimetre topography and reject very smooth surfaces (Hills and Thomason 1998). The reason may be that textured surfaces offer extra adhesion strength for bioadhesives because of increased wetted surface and possible mechanical locking. At the LCS in Elmer it was found that very smooth surfaces on the syenite building blocks were almost free from sessile epibiota like barnacles on the seaward side (Fig. 14). One prediction from this analysis is that very smooth surfaces (roughness less than 0.2 mm) on LCS building blocks can be used to minimise barnacle presence. Since barnacle shells are razor sharp this may be desirable if LCS are to be designed for recreational use.

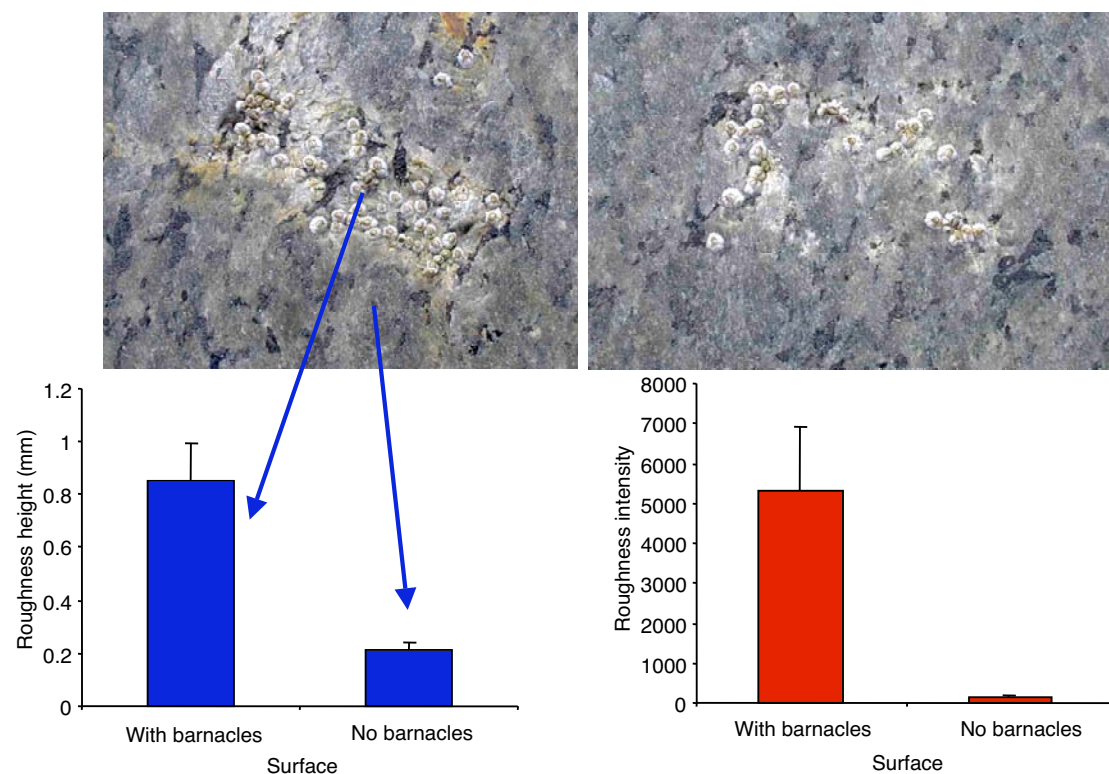


Fig. 14. Correlation between small-scale topography (roughness) and the presence of barnacles on LCS in Elmer, UK. Roughness height is the maximum difference in height across measured profiles, and roughness intensity is the power of dominant roughness scales as analysed with a FFT algorithm.

Scour

High-energy flow caused by orbital wave motion and shoaling will resuspend bottom material, from silt to large stones. The combination of resuspension and high flow

speeds, e.g. during wave breaking can lead to scour damages on the epibiota on an LCS. Scour from small particles may lead to long-term wear on tissues and hard shells, while larger pebbles may lead to instant detachment or mortality. Within DELOS two empirical studies at Elmer were performed to test for the presence of scour. The first study considered the soft-bodied macro-alga *Enteromorpha*. On the seaward side *Enteromorpha* is only found on shells of limpets (*Patella vulgata*) where they escape from grazing. Scour on an LCS is expected to be a strong function of the height above the seabed because of the Rouse distribution of negatively buoyant particles (Rouse 1937). The hypothesis was tested that the frequency of limpets with *Enteromorpha* on the shell was lower within 0.5 m of the LCS toe compared to mid-shore. Since limpets are very stationary they are expected to integrate the local scour over a long time. As seen in Fig. 15 no evidence for increased scour on limpet shells near the toe could be found.

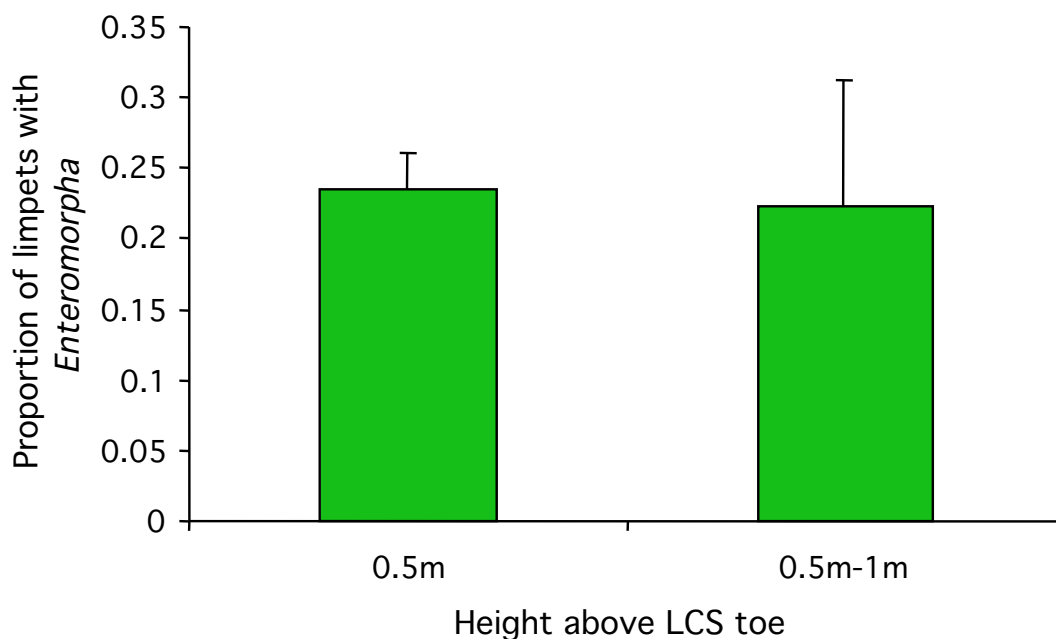


Fig. 15. Proportion of limpet shells on LCS in Elmer, UK with a cover of *Enteromorpha* sp. for two different heights above the LCS toe.

In a second study the distribution of barnacles was recorded for the first 0.5 m above the LCS toe. The hypothesis was that scour would reduce the number of barnacles close to the toe and, in particular, the older generation. Figure 16 indeed shows that there is a thin zone close to the toe (10 cm) with almost no barnacles (cover less than 1%) and an intermediate zone (20 cm) with only new recruits and an upper zone (above 40 cm) where older barnacles occur. Although other explanations for this pattern are possible, scour is a probable cause.

In conclusion, it is suggested that scour is only important for the epibiota very close to the toe (0-40 cm).

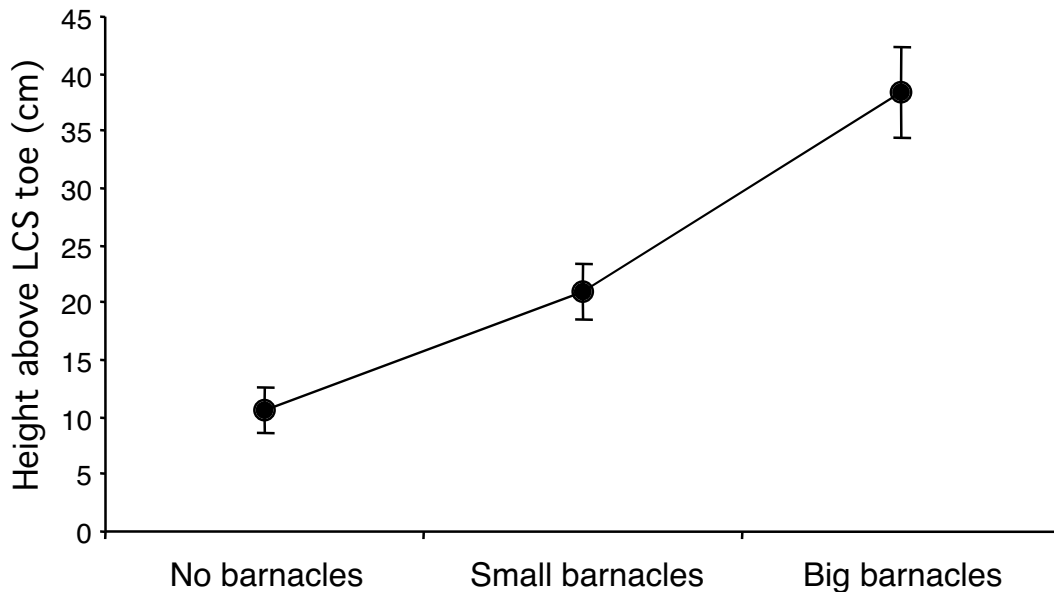


Fig. 16. Presence/absence of small recruits and adult barnacles as a function of the height above LCS toe in Elmer, UK.

Water exchange and demand for oxygen and nutrients

Most LCS are constructed with building blocks of a geometry and size distribution that lead to voids among individual blocks. The porosity and void size will affect the internal, or porous, flow within the LCS. Porous flow ranges from very low in LCS with a core of fine and unsorted material to high within LCS without a core where gaps approach the size of armour building blocks. The interior of LCS may offer suitable habitats for many marine organisms. Because light intensity is low, only heterotrophic organisms (e.g. animals) are expected within LCS. A potentially limiting factor for animals living in gaps within an LCS is the supply of oxygen and nutrients. Animals within the LCS will consume oxygen and nutrients and if this is not balanced by supply from the water flowing into the LCS interior growth and survival are affected. This may be a potential management problem if periods with high interior flows are interrupted by periods with low flows. A worst scenario is high flows and good oxygen supply during spring and early summer when many animals recruit to LCS surfaces, hydrodynamic conditions are energetic and the temperature often low. In late summer the biomass will peak and the water temperature will be high leading to high oxygen demand, while calm weather conditions lead to low internal flows. During such events the balance between oxygen demand and supply may shift and results in oxygen deficiency and mass mortality with unpleasant smell of decomposing biomass. Within DELOS WP 3.5 a simple model was formulated to explore under what conditions oxygen deficiency may be expected.

Model of LCS interior flow and biological oxygen demand

The objective is to model the oxygen balance only for epibiotic animals larger than a few millimeter. This include dominant groups like barnacles, mollusks, decapod crustaceans and fish. Consequently, only gaps in the LCS interior larger than 1 cm is considered in the model. For this minimum pore size pipe Re is generally above 2000 already for flow speeds of 0.1 m s^{-1} and flow will be turbulent for most modelled pore

sizes. To model the turbulent interior flow a simplistic strategy is chosen where the gaps are viewed as a series of pipes through the LCS, parallel to the sea surface and along the seaward-landward axis. The mean speed for turbulent flow through a pipe with radius a and length l can be expressed as (Massey 1989):

$$\bar{u} = \sqrt{\frac{4(a-D)\Delta p}{fl\rho}} \quad \text{eq. 10}$$

where Δp is the pressure drop, and f is the friction factor (here set to 0.05) and D is the thickness of the biological layer. The pressure drop can be expressed in terms of the water-level difference z across the LCS as:

$$\Delta p = zg\rho \quad \text{eq. 11}$$

A maximum biological development is considered within the pipe where a biologically active layer covers the pipe's inner surface. This biological layer (D) is assumed to respire oxygen at a rate of R (expressed as m^3 of oxygenated seawater per s). The oxygen depletion of water passing through the pipe is calculated as:

$$O_{out} = O_{in} \exp\left(-\frac{Rl}{Vu}\right) \quad \text{eq. 12}$$

where O_{in} is oxygen concentration of fully oxygenated seawater ($8000 \text{ ml O}_2 \text{ m}^{-3}$) entering the LCS and O_{out} is the oxygen concentration of the water exiting from the LCS. Oxygen deficiency within the LCS is defined as when O_{out} is below 2000 ml O_2 which results in mild hypoxia for many organisms (Rosenberg et al. 1991). The model is used to evaluate at what critical pore size the exiting oxygen concentration reached hypoxic levels. The parameters in the model are shown in Table 1.

Table 1. Parameter values in the model of oxygen balance within an LCS.

Parameter	Value(s)	Reference
LCS length (l)	10 m	
Biological layer (D)	0.01 m (barnacles), 0.05 m (mussels)	
Respiration rate (R)	$0.24 \text{ ml O}_2 \text{ g}^{-1} \text{ h}^{-1}$	Rosenberg & Loo (1983)
Sea water oxygen (O_{in})	$8000 \text{ ml O}_2 \text{ m}^{-3}$	
Oxygen level at hypoxia (O_{ex})	$2000 \text{ ml O}_2 \text{ m}^{-3}$	Rosenberg et al. (1991)
Water-level difference (z)	0.05 to 0.2 m	

Figure 17 shows how the critical pore size changes with the water-level difference (pressure head) and the thickness of the epibiotic layer. The model predicts that if the pores are sufficiently large to fit a biological layer the supply of oxygen will be less of a problem. Above a pore diameter of 0.2 m oxygen deficiency is unlikely according to the model even at the small water-level slope of 0.5 %. Some aspects of the model is rather conservative since it assumes that all available interior surface is covered with organisms and oxygen deficiency is here defined at the exit. However, other aspects probably underestimate the risk of oxygen deficiency, mainly the unreasonable assumption of no residual water within the LCS and that all oxygen is radially well mixed. It is probably also possible of having even lower pressure gradients during extremely calm conditions. In conclusion, oxygen deficiency seems unlikely for pore sizes exceeding 0.2 m.

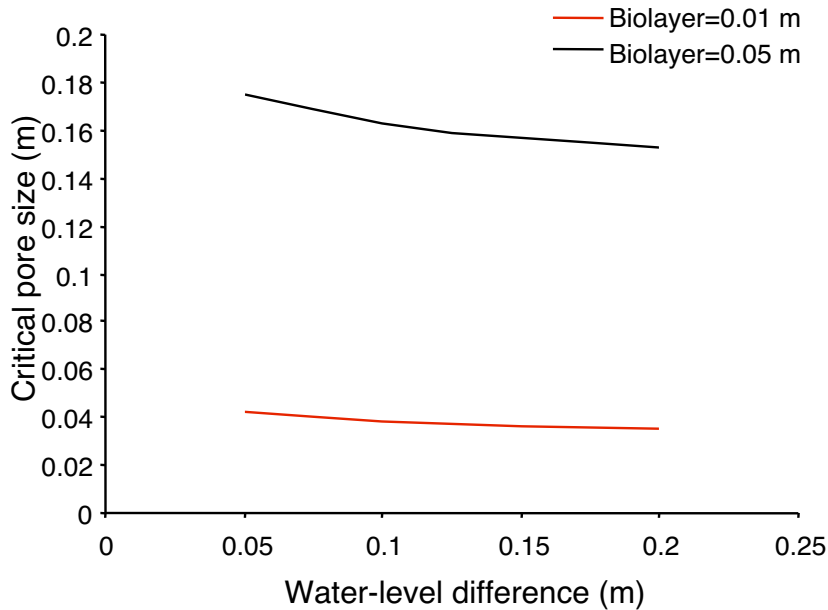


Fig. 17. Modelled critical pore size, leading to oxygen deficiency, as a function of water-level difference across an LCS with interior populations of epibiota. Two biomass levels are considered, modelled as biolayer thickness.

Model of LCS interior flow and nutrient depletion

A similar model as for the oxygen balance can be made for the flux of nutrients. Depletion of nutrients, mainly food particles for suspension feeders, will lead to slow growth but is not expected to result in the dramatic and simultaneous mortality as during oxygen deficiency. A simple model similar to eq. 12 can be formulated to estimate the minimum pore size that can support a complete cover of suspension-feeders. Respiration rate is replaced with clearing rate F (1 h^{-1}) of particles expressed as (Riisgård 2001):

$$F = 0.0012D^{2.14} \quad \text{eq. 13}$$

where D is the length of suspension-feeders (in mm), here assumed identical to the thickness of the epibiotic layer. In the model, food depletion is defined as when the food concentration in the flow entering the LCS interior has been reduced to 25% when exiting. Figure 18 shows that critical pore sizes for food depletion are similar to what was found above for oxygen deficiency.

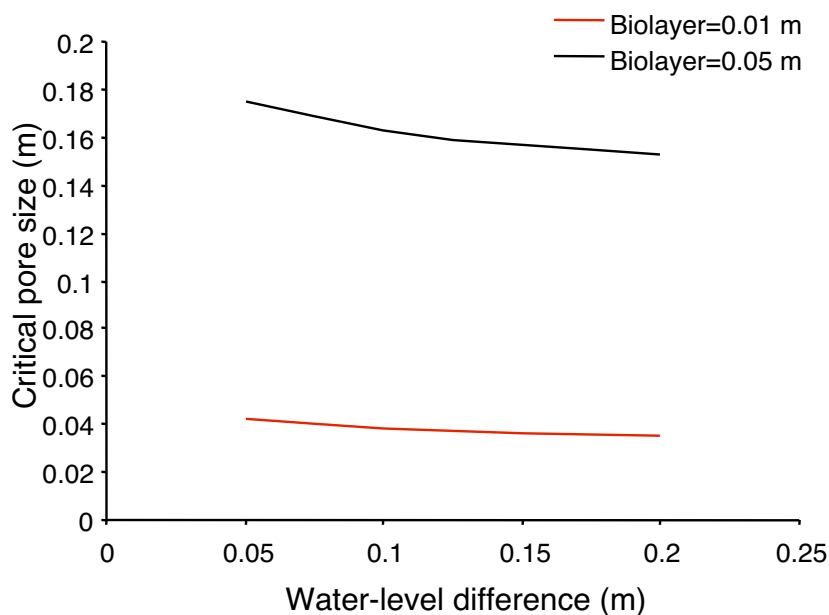


Fig. 18. Modelled critical pore size, leading to depletion of suspended food, as a function of water-level difference across an LCS with interior populations of epibiota. Two biomass levels are considered, modelled as biolayer thickness.

Statistical models of epibiotic distribution on LCS

General patterns of landward and seaward side differences

Another model approach, compared to the hydrodynamic model above, is to use statistical models to predict the development of epibiota on LCS. The strength of statistical models is that they do not rely on any in-depth knowledge of the processes generating observed patterns. The obvious disadvantage is their often poor ability to predict patterns for new conditions (extrapolation). From the distribution data on epibiota collected within WP 3.2 it is possible to test for significant patterns on the LCS. The totally dominant statistical factor (within the scale of LCS) is the landward-seaward sides. Many epibiotic species show marked differences in their distribution between the landward and the seaward sides. Figures 19 and 20 show an overall picture of how the species composition differs for both Elmer in UK and the Adriatic Sea in Italy. A simple overview of the differences between the landward and the seaward side is found in Table 2 (more detailed information is found in the report of deliverable D35 in WP 3.2). Table 2 shows that some species are almost entirely found on one of the sides of an LCS and that the differences may be more the 10-fold. There is a general tendency that macro-algae dominate on the landward side. This may be in part driven by hydrodynamic effects as suggested by the hydrodynamic model above. However, it may also be an effect by the local grazing pressure. The unexpected high abundance of *Enteromorpha* sp. and *Ralfsia* found on the seaward sides on LCS in Lido Adriano may be an effect of the near absence of limpets. This shows that accurate predictions of local epibiota depends on both hydrodynamic and biological processes.

Table 2. Summary of main differences in species composition between the landward and the seaward sides in Elmer, UK and on the Adriatic coast, Italy. The abundance is expressed in percent cover.

English Channel

Elmer

	Landward	Seaward	Ratio LW/SW
<i>Balanus</i> spp.	16	16	1.0
<i>Littorina</i> spp.	1.5	0.3	5.0
<i>Patella vulgata</i>	0.3	0.8	0.4
<i>Fucus vesiculosus</i>	5	0	large
<i>Enteromorpha</i> spp.	7	0	large

Adriatic Sea

Lido di Adriano

	Landward	Seaward	Ratio LW/SW
<i>Balanus</i> spp.	0	2	small
<i>Mytilus</i> spp.	8	10	0.8
Oysters	10	5	2.0
<i>Patella</i> spp.	0.05	0.2	0.3
<i>Ralfsia</i> sp.	4	5.5	0.7
<i>Enteromorpha</i> spp.	1.8	11	0.2

Adriatic Sea

Cesenatico

	Landward	Seaward	Ratio LW/SW
<i>Balanus</i> spp.	1.5	15	0.1
<i>Mytilus</i> spp.	45	76	0.6
Oysters	15	1	15
<i>Patella</i> spp.	4	3	1.3
<i>Ralfsia</i> sp.	4	0.6	6.7
<i>Enteromorpha</i> spp.	0	0	1

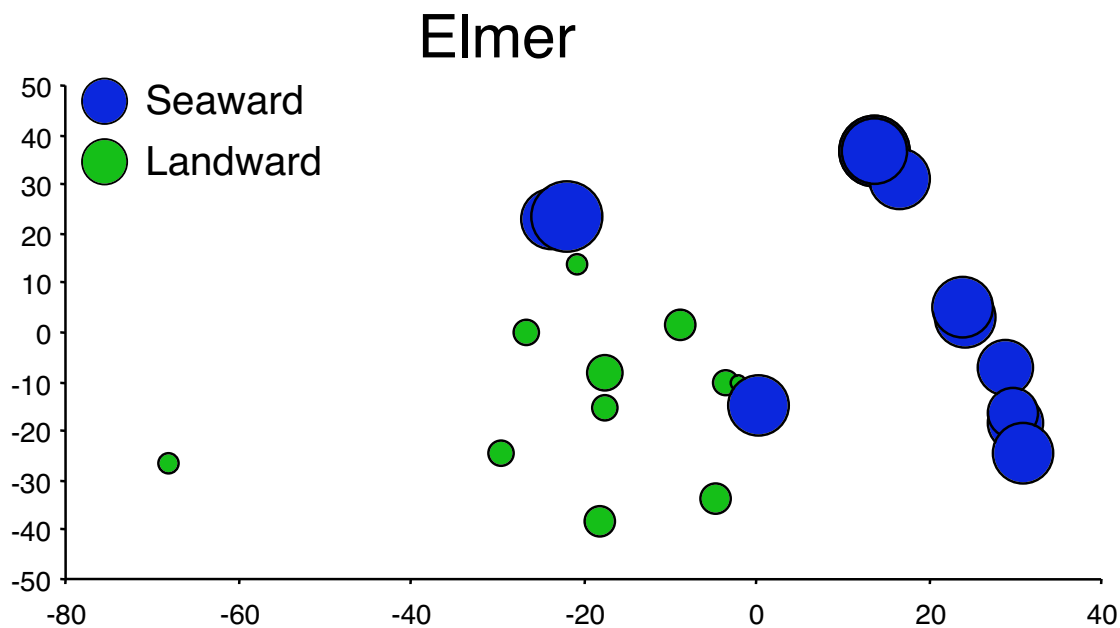


Fig. 19. Multidimensional scaling plot of how the species composition differs between landward and seaward sides of LCS in Elmer, UK. The size of markers indicates the magnitude of flow speeds measured as erosion of gypsum. Values shown on the x- and y-axis are arbitrary and only indicate the projected 2-dimensional distance between stations based on the multivariate species composition.

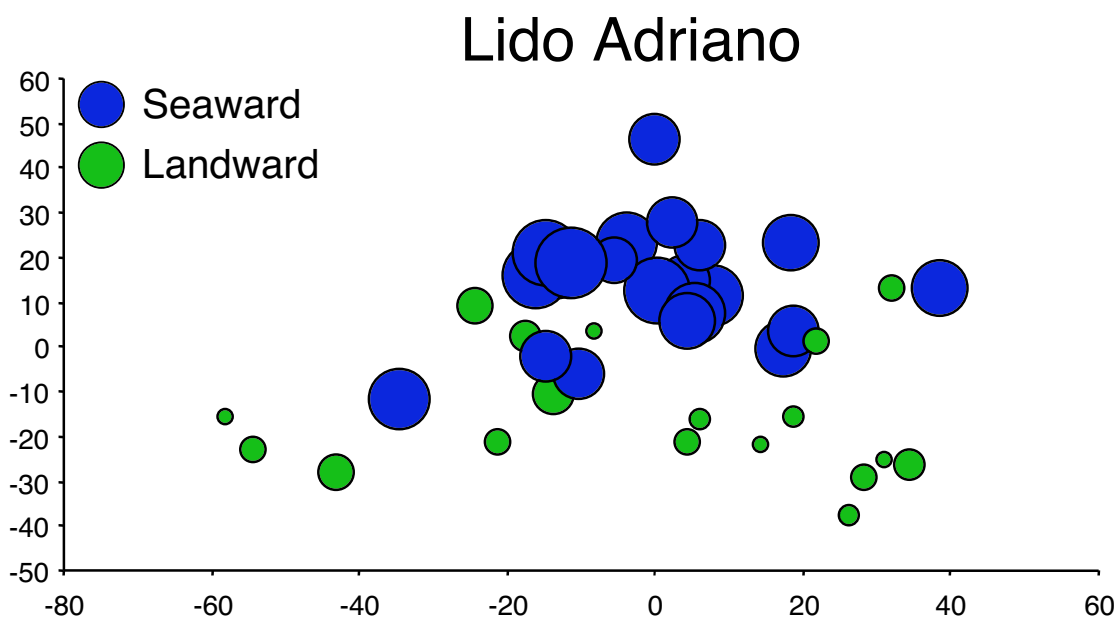


Fig. 20. Multidimensional scaling plot of how the species composition differs between landward and seaward sides of LCS in Lido Adriano, Italy. The size of markers indicates the magnitude of flow speeds measured as erosion of gypsum. Values shown on the x- and y-axis are arbitrary and only indicate the projected 2-dimensional distance between stations based on the multivariate species composition.

Patterns on smaller scales

Along LCS gradients

Apart from the clear difference of epibiota between the landward and the seaward sides of LCS there were additional small-scale patterns along the LCS. On the landward side several species showed along LCS gradients. Figure 21 shows that barnacles decline from east to west on two studied LCS. *Fucus vesiculosus* and *Enteromorpha* sp. show peak abundance in the middle of the studied transect. The barnacle gradient corresponds to a decline in average flow speed as measured with gypsum discs (Fig. 21). On the seaward side there are no clear along LCS gradients.

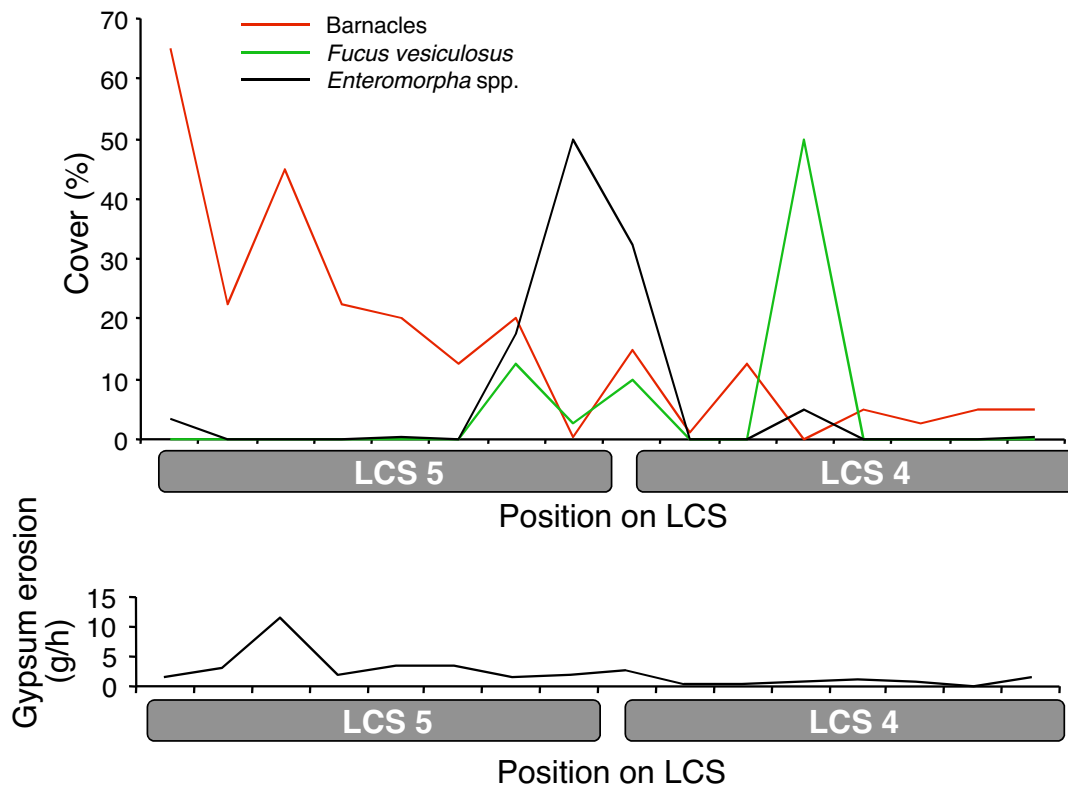


Fig. 21. Gradients in epibiotic species abundance along two LCS in Elmer, UK. The lower panel shows differences in gypsum erosion along the LCS on the landward side.

Horizontal and vertical rock faces

A very clear pattern in Elmer is the difference in barnacle abundance on horizontal and vertical faces of LCS building blocks. Figure 22 shows how the presence of barnacles is a strong function of the inclination of the rock face. When the inclination is over 100° barnacles almost disappear. A hypothetical explanation is that flow is too fast over rock faces above a certain inclination. A test with gypsum discs indicates that flow speed is indeed a function of face inclination (Fig. 22).

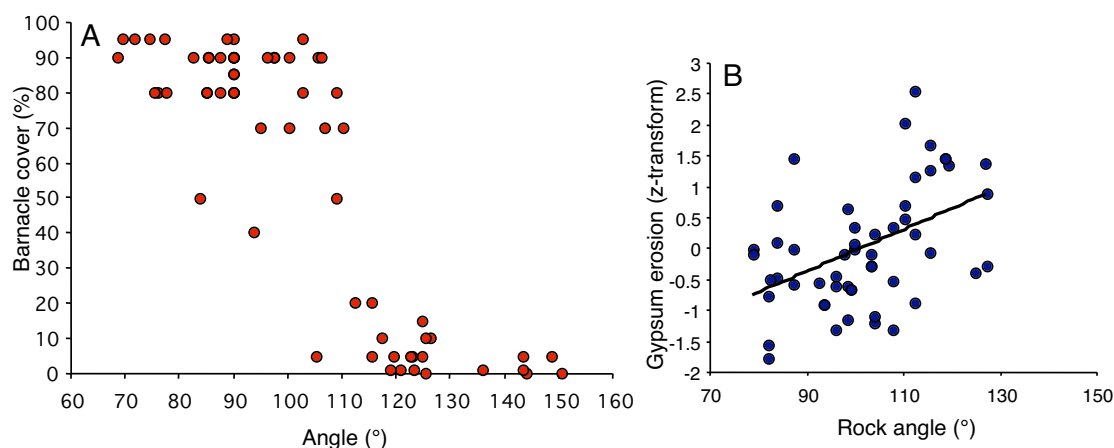


Fig. 22. (A) Barnacle cover as a function of the rock face inclination on the seaward side on LCS in Elmer, UK. Inclinations above 90° indicates rock faces sloping from the seaward and in against the LCS. (B) Positive correlation between rock inclination and average flow speed as measured as gypsum erosion.

Conclusions

This deliverable (D48) focuses on detecting and predicting patterns of epibiota on LCS in relation to the hydrodynamic environment. From field work together with statistical and theoretical analyses the following conclusions about identified relations between epibiotic patterns and hydrodynamic regime can be made:

1. The survival of epibiotic organisms may depend on rare events of maximum wave-induced forces. The maximum force acting on epibiota, and thus probability of detachment, is expected to be approximately linearly related to maximum breaking wave height.
2. Hydrodynamic forces, modelled and observed, acting on the epibiota on LCS can be sufficiently large to detach organisms or inflict tissue damages.
3. Topography on scales larger than epibiota will offer refuges increasing survival and biodiversity
4. Topography on scales smaller than epibiota may be important during recruitment and for adhesion strength. Very smooth surfaces, in particular in combination with high flow speeds, can be used to reduce the diversity and abundance of epibiota.
5. Scour on the observed LCS seems to be a problem for epibiota only in a zone close to the toe.
6. A model of flow within LCS indicates that the supply of oxygen is sufficient to support macro-fauna for pore sizes exceeding 0.2 m.
7. A model of flow within LCS indicates that the food supply is not significantly reduced if pore size exceeds 0.2 m.

References cited

- Anonymous. 1989. Engineering and design - water levels and wave heights for coastal engineering design. EM 1110-2-1414. US Army Corps of Engineers
- Bell EC, Denny MW. 1994. Quantifying wave exposure - a simple device for recording maximum velocity and results of its use at several field sites. *J Exp Mar Biol Ecol* 181: 9-29

- Blanchette CA. 1997. Size and survival of intertidal plants in response to wave action: a case study with *Fucus gardneri*. *Ecology* 78: 1563-1578
- Denny MW, Miller LP, Stokes MD, Hunt LJH, Helmuth BST. 2003. Extreme water velocities: Topographical amplification of wave-induced flow in the surf zone of rocky shores. *Limnol Oceanogr* 48: 1-8
- Denny MW. 1988. *Biology and the mechanics of the wave-swept environment*. Princeton University Press, Princeton.
- Denny MW, Daniel TD, Koehl MAR. 1985. Mechanical limits to size in wave-swept organisms. *Ecol. Monogr* 55: 65-102
- Goda Y. 1985. *Random sea and design of maritime structures*. Univ Tokyo Press, Tokyo
- Hills JM, Thomason JC (1998) The effect of scales of surface roughness on the settlement of barnacle (*Semibalanus balanoides*) cyprids. *Biofouling*. 12: 57-69
- Lewis JP. 1968. Water movements and their role in rocky shore ecology. *Sarsia* 34: 13-36
- Massey BS. 1989. *Mechanics of fluids*. Van Nostrand Reinhold, London
- Porter ET, Sanford LP, Suttles SE. 2000. Gypsum dissolution is not a universal integrator of 'water motion'. *Limnol Oceanogr* 45: 145-158
- Rouse H. 1937. Modern concepts of the mechanics of turbulence. *Trans Am Soc Civ Eng* 102:463-643.
- Riisgård HU. 2001. On the measurement of filtration rates in bivalves-the stony road to reliable data: review and interpretation. *Mar Ecol Prog Ser* 211:275-291.
- Rosenberg R, Hellman B, Johansson B. 1991. Hypoxic tolerance of marine benthic fauna. *Mar Ecol Prog Ser* 79: 127-131
- Rosenberg R, Loo L-O. 1983. Energy flow in a *Mytilus edulis* culture in western Sweden. *Aquaculture* 35: 151-161

Appendix

Code (MatLab, MathWorks Inc) for model of wave-induced forces on epibiota (*Fucus vesiculosus* and *Littorina littorea*).

```
% The code calculates shallow-water wave height from a wave-buoy time series of
% deep-water waves (Station Owers). The shallow-water wave height is compared to
% the max breaking height to determine if an LCS will receive the breaker or if
% the wave will be broken off-shore. If the LCS receives the breaker a maximum
% flow velocity for breakers is calculated. From this flow speed a maximum
% hydrodynamic force is calculated for Littorina snails or for Fucus macro-algae.
% This maximum drag force is compared to empirically found adhesion forces to
% determine the probability of detachment from the LCS substrate.
```

```
clear all
clf
```

```
% input of constants
g=9.81; % acceleration of gravity
h=4; % the maximum depth of the lower part of the LCS (at high tide)
slope=1/10; % from Elmer data
littorina_area=(24/1000/2)^2*pi;
littorina_volume=(24/1000)^3*pi/6;
```

```

fucus_volume=0.02/1000;
flow_acceleration=400; % Blanchette (1997)

% for wave-induced flow speeds for landward side the variable below is set to the
% empirically found relationship (0.16) between maximum flow speeds on the
% landward and seaward side
seaward_landward=1;

% loading of wave-buoy time series. The data consists of day No, Hs and period
load wavebuoy2.m;
wave_series=wavebuoy2;
[row,column]=size(wave_series);
wavelength=g.*wave_series(:,3).^2./2./pi;
k=2*pi./wavelength;

% Dimensioning
report=zeros(row,3);

% calculating breaking wave height
breaking_height=0.18.*wavelength.*(1-exp(-
1.5.*pi.*h./wavelength.*(1+15.*slope^1.33)));

% calculating shallow-water wave height
shallow_height=wave_series(:,2).*sqrt(sinh(2*h.*k)./(sinh(2*h.*k)+2*h.*k)./tanh(k.*
h));

% comparing shallow-water wave height with breaking wave height, and setting all
% events to zero where shallow-water height exceeds breaking height
I=shallow_height<breaking_height;
impact_height=I.*shallow_height;

% calculating maximum flow speed in wave breaking on the LCS
flow_max=seaward_landward.*sqrt(2*g.*impact_height);

% calculating maximum drag force and acceleration reaction on Fucus using an
% empirical relationship between flow speed and drag, and weight data on Fucus for
% acceleration reaction
drag_fucus=0.2266.*(flow_max+.05).^1.498;
reaction_fucus=1024.*2.*flow_acceleration.*fucus_volume.*seaward_landward;
total_fucus=drag_fucus+reaction_fucus;

% calculating maximum drag and lift forces on Littorina snails
drag_littorina=0.5.*0.5.*1024.*littorina_area.*flow_max;
reaction_littorina=1024.*2.*flow_acceleration.*littorina_volume.*seaward_landward;
lift_littorina=0.5.*0.5.*1024.*littorina_area.*flow_max;
total_littorina=sqrt((drag_littorina+reaction_littorina).^2+lift_littorina.^2);

% Plotting data
figure(1)
plot(total_fucus)

```

```
figure(2)  
plot(total_littorina)
```

```
% Saving data to file
```

```
report(1:row,1)=flow_max;  
report(1:row,2)=total_fucus;  
report(1:row,3)=total_littorina;  
save results report -ascii -double -tabs
```